Green Chemistry

PAPER

View Article Online
View Journal | View Issue

Cite this: *Green Chem.*, 2025, **27**, 527

Green synthesis of poly ε-caprolactone using a metal-free catalyst *via* non-covalent interactions†

Shweta Sagar, [a] Priyanku Nath, [a] Shiva Lall Sunar, [a] Aranya Ray, [a] Mridula Choudhary, [a] Alok Sarkar, *[b] Saurabh K. Singh *[a] and Tarun K. Panda *[a]

Received 3rd September 2024,
Accepted 18th November 2024

DOI: 10.1039/d4gc04411h

rsc.li/greenchem

The ring-opening polymerization (ROP) of ε-caprolactone (CL) catalyzed by a metal-free initiator *N*,*N*′-dibutyl-*N*,*N*,*N*′,*N*′-tetramethylethane1,2-diammonium bromide [^{n}BuMe$_2$NCH$_2$CH$_2$N^{n}BuMe$_2$]Br$_2$ (DBTMEDA)Br$_2$ has been investigated. The catalyst (DBTMEDA)Br$_2$ promotes polymerization under mild conditions without any external initiator. Polymerization was demonstrated in a controlled and living manner, producing PCLs with a precisely controlled molecular weight of up to 50 kDa with narrow polydispersity. Density Functional Theory (DFT) calculations indicated the involvement of a C–H···O type non-covalent interaction between DBTMEDA cations and the carbonyl group of ε-CL in the monomer activation step. Remarkably, DBTMEDA can also be easily recovered and reused for up to six consecutive cycles without an appreciable decrease in catalytic activity.

Introduction

Green chemistry aims to increase the usage of monomers from natural resources and implement safer, more efficient, and eco-friendly chemical processes. Non-covalent interactions, even though very weak in nature, play a dominant role in pharmaceutical design, supramolecular chemistry, molecular biology, sensing applications, material and crystal engineering, and a host of other fields in the chemical sciences.[1–6] Immense efforts have been put forth by theoretical as well experimental scientists to quantitatively establish the role of non-covalent interactions, which include hydrogen bonding, electrostatic effects, π–π, cation–π, and hydrophobic interactions, and van der Waals forces.[7–12] Notable contributions of these forces to rate accelerations and stereoselectivities have also been exemplified in several enzymatic catalyses.[13,14] In a similar direction, Zhao and coworkers have leveraged the strong hydrogen-bonding ability of a commercially available fluorinated alcohol to perform efficient ROP of α-amino acid *N*-carboxyanhydrides with no cocatalyst.[15]

Poly(ε-caprolactone) (PCL) is a high-demand synthetic polyester with attractive features such as excellent biodegradability, biocompatibility, good thermal stability, and ease of manufacture.[16] Since the first synthesis of PCL by the Carothers group in the early 1930s, various PCL polymers have been commercialized and applied in many fields today, ranging from the biomedical and pharmaceutical fields to the agricultural field. Recently, with the advancement of tissue engineering, there has been a strong surge in demand for PCL, with the total estimated volume expected to reach 909.81 billion USD by 2029.[17] Compared to the traditional polycondensation methods, metal complex-induced ring-opening polymerization (ROP) of ε-caprolactone (ε-CL) is more effective and provides better controllability for the production.[18]

Numerous well-defined discrete metal complexes have been developed for the ROP of ε-CL.[19–26] However, the presence of traces of metal residues in commercial products is one of the challenges in using these polymers in biomedical, drug delivery, tissue engineering, and micro-electronics applications.[27–30] Both organocatalysts and enzymes have been intensively investigated for the ROP of cyclic esters as alternative metal-free catalysts.[31–35] Enzyme catalysts demonstrate high selectivity and promising catalytic activity under mild reaction conditions.[36] However, enzyme-catalyzed industrial processes still face the challenge of improving the reactivity of enzymes in non-aqueous media. To overcome these problems, difunctional systems combining an H-bond donor compound with an organic base (H-bond acceptor) have been designed.[37–41] In this approach, the ester moiety of the cyclic monomer is activated by the H-bond donor. Concomitantly, the base accepts an H-bond from an externally added alcohol to initiate the polymerization. Besides the desired H-bond

[a]*Department of Chemistry, Indian Institute of Technology Hyderabad, Kandi – 502 284, Sangareddy, Telangana, India. E-mail: tpanda@chy.iith.ac.in, sksingh@chy.iith.ac.in*
[b]*Momentive Performance Materials Pvt. Ltd, Survey No. 09, Hosur Road, Electronic City (west), Bangalore-560100, India. E-mail: alok.sarkar@momentive.com*
† Electronic supplementary information (ESI) available. See DOI: https://doi.org/10.1039/d4gc04411h

association with the monomer and initiating alcohol, the H-bond donor and acceptor compounds can interact, which may represent a limitation of a difunctional H-bond donor catalyst. Such interactions lowering the amount of the active catalyst in solution or even completely quenching the catalytic activity have been reported.[42,43]

Ionic liquids (ILs) as organocatalysts are one of the hot topics of chemistry in catalysis research. ILs are liquid compounds of cations and anions that display ionic-covalent crystalline structures.[44] Significant features of ILs that make them suitable as catalysts are their flexibility of adjusting acidity/basicity by simple cation/anion exchange reactions.[45–48] Despite the widespread utility of ILs in various inter-disciplinary areas of fields, their application in ROP of ε-CL remained limited to only specific aromatic imidazolium-salt containing alkyl chains such as 1-butyl-3-methylimidazolium hexafluorophosphate [Bmim][PF_6], 1-methyl-3-methyl-imidazolium hexafluorophosphate [Memim][PF_6] and bis(*N*-(*N*′-butylimidazolium)alkane) (Fig. 1).[49–51] Also, these ILs are of high cost and environmentally toxic and have high purity requirements.[52–54] High temperature, slow reaction, and requirement of an external initiator remain the critical disadvantages of these organocatalysts compared to conventional metal catalysts.

On the other hand, aliphatic quaternary-ammonium-salts containing alkyl chains exhibit stronger ionic interactions because of their localized cationic charge on the ammonium group and enhanced van der Waals interactions among the alkyl chains.[55] Therefore, we anticipated that they might enable faster ROP by their stronger ionic interaction with the monomer than their aromatic imidazolium counterparts. As catalysts for ROP, aliphatic quaternary-ammonium-salts can present numerous other advantages, including their green character, simple one-step synthesis from readily available commercial materials, and ease of handling. Furthermore, their characterization and solution properties have been well established,[55–57] but to the best of our knowledge, their application as catalysts for the ROP is unknown. Herein, we describe our study of an aliphatic dicationic quaternary ammonium salt, DBTMEDA (**1**), catalyzing the ROP of ε-CL (Fig. 1). Syntheses of PCL with precise and predictable control over the molecular weight were achieved with >95% conversion within 8 h under mild reaction conditions. The catalyst recovery and reusability studies performed on a representative reaction demonstrated efficient recycling of the catalyst. We also present a model in which a non-covalent interaction, namely the C–H···O hydrogen bond, between the carbonyl group of ε-CL and a methylene CH_2 group of dicationic ammonium salts triggers monomer activation to initiate the polymerization.

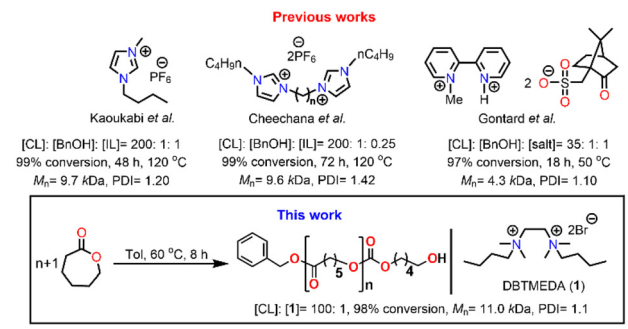

Fig. 1 Previously reported organocatalysts and the current work for ROP of ε-CL.

Results and discussion

Synthesis of salt

The salt *N*,*N*′-dibutyl-*N*,*N*,*N*′,*N*′-tetramethylethane-1,2-diammonium bromide (**1**) was synthesized using a procedure reported in the literature.[55]

Ring-opening polymerisation of ε-CL

The catalytic activity of **1** was first verified for the ROP of 100 equivalents of ε-CL at 60 °C using toluene as the solvent (Table 2). It was intriguing to note that a 37.6% conversion in the first two hours was observed without any external initiator. With this encouraging finding, a first screening was conducted to find the optimal time for the complete conversion without any external initiator. Upon further proceeding with the reaction, 58.8, 79.9, and 98.3% conversions were attained in 4, 6, and 8 h, respectively. After quenching with BnOH, 99% of the polymer product was isolated by precipitating the crude reaction mixture in water. The solvent toluene was recovered from water using a separating funnel. The turnover frequency (TOF) calculated for the catalyst was 12.2 h^{-1}, substantially higher than the value calculated for the same reaction reported using an ionic liquid-based catalyst (Table 1). Even though the highest TOF of 13.3 h^{-1} could be achieved in the first 6 h, the polymerization was continued for 8 h to ensure >95% monomer conversion. The other green chemistry metrics evaluated for this reaction such as *E*-factor, atom economy (AE), atom efficiency, carbon efficiency (CE), product mass intensity (PMI), effective mass yield (EMI) and reaction mass efficiency (RME) were also improved significantly compared to the reported IL catalyst (Table 1). Fig. FS10 in the ESI† shows the ^{1}H NMR spectrum of the prepared PCL showing the typical peaks as reported in the literature.[25] The chemical shifts of 4.07, 2.29, 1.64, and 1.34 ppm are due to PCL, and the peak due to the methylene protons adjacent to the ω-chain end of the hydroxyl group is observed at 3.65 ppm. The chemical shifts of 7.32 and 5.10 ppm are due to the aromatic methylene protons of the BnO^- moiety attached to an ester linkage, respectively. Additionally, the number-average molecular weight of the polymer estimated from ^{1}H NMR agreed with that calculated from the feed monomer to initiator ratio and monomer conversions (Table 2, entry 4).

The monomer-to-catalyst ratio plays a crucial role in the ROP of cyclic esters. Next, we carried out the polymerization by successively increasing the monomer loading to 200, 300, 400, and 500 equivalents at a given catalyst concentration. High conversions of the monomer were achieved for all the reactions to give

Table 1 The comparison of green metric parameters for the ROP of ε-CL using ionic liquids (previous work in the literature) and salt (present study)

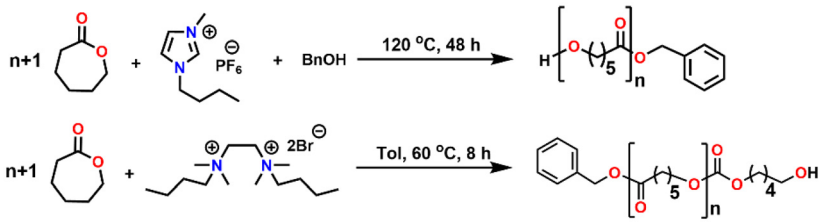

Green chemistry metric	Acronym formula	Ref.	Previous approach	Current work
E-factor	$E\ \text{Factor} = \frac{\text{Total mass of waste}}{\text{Mass of Product}}$	67 and 68	0.5	0.01
Atom economy (AE)	$\text{AE} = \frac{\text{MW of product}}{\sum \text{MW of reactants}} \times 100$	67 and 68	98%	100%
Atom efficiency (AE)	$\text{AE} = \frac{\%\ \text{yield of product} \times \%\ \text{AE}}{100}$	67 and 68	98%	99%
Carbon efficiency (CE)	$\text{CE} = \frac{\text{No. of carbon atoms in product}}{\sum \text{No. of carbon atom in product}} \times 100$	67 and 68	100%	100%
Product mass intensity (PMI)	$\text{PMI} = \frac{\sum \text{Mass of reactants including solvent}}{\text{Mass of Product}}$	67 and 68	1.5	1.02
Reaction mass efficiency (RME)	$\text{RME} = \frac{\text{Mass of product}}{\sum \text{mass of reactants}} \times 100$	67 and 68	66%	98.9%

Table 2 ROP of ε-CL by salt[a]

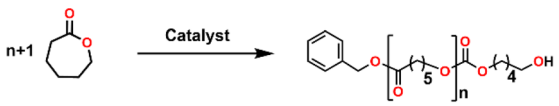

Entry	Cat : M	Cat (mol L^{-1})	Monomer (mol L^{-1})	Time (h)	Temp. (°C)	Conv.[b]	Yield[c]	TON[d]	TOF (h^{-1})[e]	$M_{n\ theo}$[f] (kDa)	$M_{n\ exp}$[g] (kDa)	PDI
1	1 : 100	0.006	0.64	2	60	37.6	21	20.7	10.3	4.4	3.1	1.6
2	1 : 100	0.006	0.64	4	60	58.8	48	47.3	11.8	6.8	5.9	1.4
3	1 : 100	0.006	0.64	6	60	79.9	81	79.8	13.3	9.2	8.8	1.3
4	1 : 100	0.006	0.64	8	60	98.3	99	97.5	12.2	11.3	11.0	1.1
5	1 : 200	0.006	1.28	8	60	98.1	99	198	24.8	22.5	21.9	1.1
6	1 : 300	0.006	1.95	8	60	97.8	98	294	36.8	33.6	33.1	1.2
7	1 : 400	0.006	2.6	8	60	96.7	97	388	48.5	44.3	43.5	1.2
8	1 : 500	0.006	3.25	8	60	95.5	96	480	60	54.6	51.6	1.4
9	0 : 100	0	0.64	8	60	0	0			—	—	—
10[h]	1 : 100	0.006	0.64	8	60	22.5	14	13.7	1.7	Nd	nd	nd

[a] In toluene, [catalyst] = 0.026 mmol. [b] Conversions were determined by crude mixture ^{1}H NMR spectroscopy. [c] Yield = (weight of the polymer obtained/weight of the monomer used) × 100. [d] TON = [(mol epoxide/mol catalyst) × isolated polymer yield (%)]. [e] TOF = TON/time (h). [f] $M_{n\ (theo)}$ = molecular weight of chain-end + 114 $g mol^{-1}$ × (salt: M) × conversion. [g] In THF (2 mg mL^{-1}) and molecular weights were determined by GPC-LLS (flow rate = 0.5 mL min^{-1}). Universal calibration was carried out with polystyrene standards, laser light scattering detector data, and a concentration detector. Each experiment is duplicated to ensure precision. [h] In THF as the solvent.

PCLs with precisely controlled molecular weights. Effective utilization of the catalytic species at the molecular level was confirmed for all reactions by their high turnover number (TON = 97 to 488). The GPC analysis confirmed a narrow molecular weight distribution (PDI = 1.1 to 1.4), indicating side reactions; for example, the transesterification, which became more predominant at high temperatures and low monomer concentrations, is restricted. As shown in Fig. FS9 in the ESI,† the average molecular weight (M_n) obtained for the polymers showed a linear dependency on the monomer-to-catalyst ratio, indicating the single-site, living behavior of the catalytic species. The influence of solvent on the polymerization was also examined (Table 2). Good control of the polymerization was observed in toluene. Polymerization in the presence of THF as a solvent was extremely sluggish, where a conversion of up to 22.5 percent could be obtained in 8 hours (Table 2, entry 10). The competitive interactions of THF with the catalyst molecule could cause a sluggish reaction in the presence of the THF solvent.

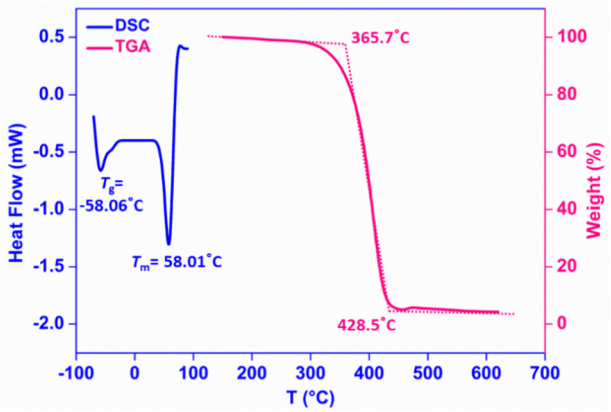

Fig. 2 DSC and TGA curves of PCL samples (entry 4, Table 1).

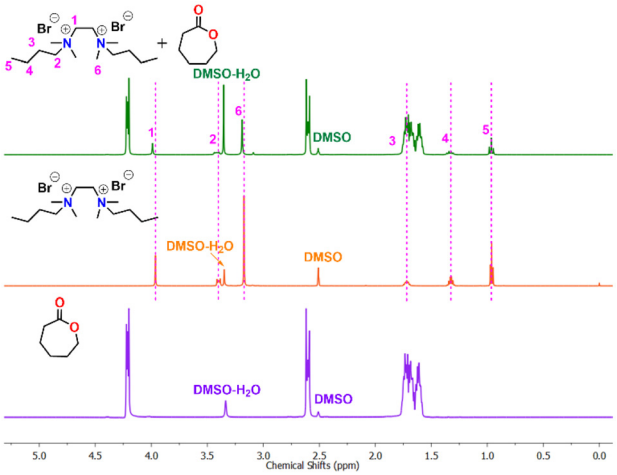

Fig. 3 ^{1}H NMR spectra of complex formed *in situ* in the mixture of salt **1** and ε-CL in DMSO.

Differential scanning calorimetry (DSC) and thermogravimetric analysis (TGA) have often been helpful to gain valuable structural insights into PCL and determine its purity and stability. The DSC thermogram of a representative polymer (Table 2, entry 4) showed the glass transition temperature (T_g) to be −58.06 °C and the melting temperature (T_m) to be 58.01 °C, which is typical behavior of conventional pure PCL (Fig. 2). Under a nitrogen atmosphere, the TGA curve of the PCL sample displayed a one-step degradation, a single weight loss phenomenon, corresponding to pyrolysis of pure commercial grade PCL.[58] The initiation of degradation was found to occur at 365.5 °C, and the final degradation temperature (T_f) was 428.5 °C with a maximum decomposition peak at 410.2 °C (T_{max}) (Fig. 2).

Having established the catalytic activity of **1** in ROP of ε-CL, we further investigated the polymerization behavior to understand the kinetics. The kinetic plots of $[CL]_0/[CL]$ *versus* the catalyst (**1**) were found to be linear, indicating first-order dependence on the ε-CL concentration (Fig. FS3 in the ESI†). The first-order dependence of the polymerization reactions substantiates the presence of only one initiator and, consequently, follows the second-order rate law, which can be expressed as rate = $-d[CL]/dt = k_p[cat]^1[CL]^1$. The activation parameters for the ROP of ε-CL in $CDCl_3$ were found to be $\Delta H^\ddagger$ = 10.8 kJ mol^{-1} K, $\Delta S^\ddagger$ = −0.14 kJ (mol K)$^{-1}$, and $\Delta E_a^\ddagger$ = 13.5 kJ mol^{-1}. The $\Delta G^\ddagger$ value for the ROP of ε-CL catalyzed by **1** at 60 °C was calculated to be 57.4 kJ mol^{-1}.

Therefore, the rate expression can be summarized as

$$-d[CL]/dt = k_{app}[Salt]^1[CL]^1 \quad (1)$$

$$-d[CL]/dt = k_{obs}[CL]^1 \quad (2)$$

where $k_{obs} = k_{app}[Salt]^1$.

The mechanism for cyclic ester ROP of various organocatalysts has been extensively investigated.[59–66] Our NMR results demonstrate the presence of the benzyl ester end group in the polymer chain when benzyl alcohol is used as a quenching agent, indicating that the ring-opening of ε-CL takes place through cleavage of the C(acyl)–O bond (Fig. FS10 in ESI†).

From the ^{1}H NMR spectra of a 1 : 10 catalyst to CL mixture, the resonance signals of CH_3 (1), CH_2 (2), and CH_2 (3) were noted to be deshielded to slightly higher chemical shift positions. In contrast, the other two signals corresponding to CH_3 (6) and CH_2 (5) remained unchanged (Fig. 3).

The observed deshielding of these specific sets of CH_3 and CH_2 protons is significant and caused by C–H···O hydrogen bonding with the carbonyl group of the ε-CL monomer. The chemical shift of CH_2 (4) could not be determined due to its overlap with other CH signals from active polymer chains. Inspired by the above observation, we anticipated that the methyl/methylene groups directly attached to quaternary ammonium groups are involved in CH_3···O=C type interactions with the carbonyl group of the ε-CL monomer. The formation of such non-covalent interactions in a similar system containing quaternary ammonium salt and a cyclic ester is also reported in the literature.[51] These non-covalent interactions increase the electrophilicity of the ε-CL monomer and it subsequently becomes susceptible to nucleophilic attack. The bromide anion, which remains as an ion pair close to the quaternary ammonium group, is considered to initiate the polymerization by the nucleophilic attack on the carbonyl-carbon of ε-CL followed by acyl–oxygen bond scission. This leads to the formation of an acyl bromide at one end of the polymer chain and active oxyanion species at the other end, which reacts with the second monomer for further propagation. Upon adding a quenching agent such as BnOH, the ester is formed as one of the end groups by nucleophilic displacement of the bromide anion from the acyl bromide. Hence, the proposed activation mechanism for ε-CL ring opening catalyzed by (DBTMEDA)Br_2 is shown in Fig. 4.

DFT studies of the ROP process

Previously, the role of CH···O=C interactions between an imidazole salt and cyclic esters has been substantiated computationally for the ROP of cyclic esters.[51] We have carried out

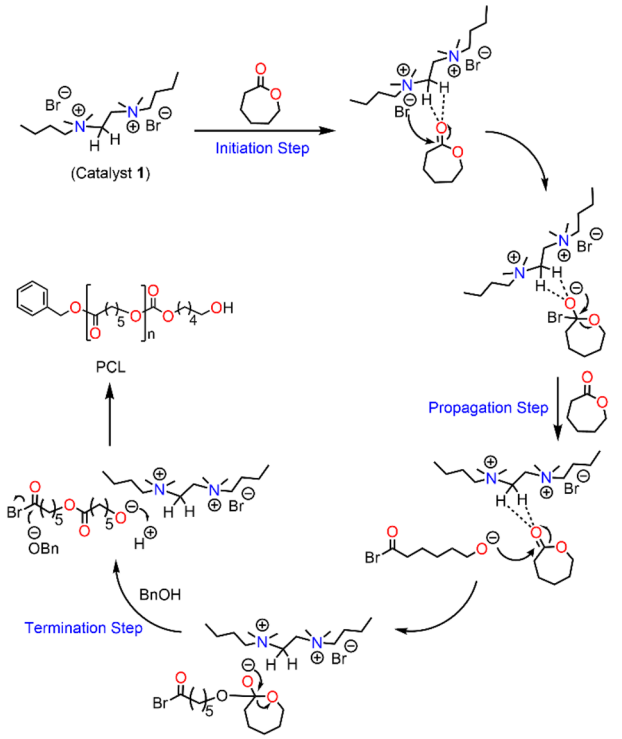

Fig. 4 Proposed mechanism of *N,N′*-dibutyl-*N,N,N′,N′*-tetramethylethane-1,2-diammonium bromide catalysed ROP of ε-CL.

geometry optimization at the B3LYP/6-31G** [69–72] levels on mixtures of ε-CL and a cationic catalyst in the absence of the counter ion. Here, we have analyzed two possible mixtures of ε-CL and a cationic catalyst, which possess different orientations of these species (**A** and **B**). Although these calculations are not directly related to the experimental observation of the ROP, the number of possible interactions present in the DFT-optimized mixtures can directly relate to the activation of ε-CL. In species **A**, we have observed that the O atom (C═O) of ε-CL is involved in the hydrogen bonding interactions with quaternary ammonium dicationic salt, where we observed one strong hydrogen bond (O1–H1) = 1.98 Å and three additional weak interactions, *i.e.* (O1–H2 = 3.08 Å, O1–H3 = 2.33 Å, and O1–H4 = 2.46 Å Fig. 5a). In contrast, we do not observe any possible hydrogen bonding interaction in species **B**, which is optimized by keeping ε-CL and quaternary ammonium dicationic salt side by side. Next, we analyzed the hydrogen bonding interaction using the non-covalent interaction (NCI) plot in **A** and **B**, where high-density NCI regions represent the hydrogen bonds while the weak interactions extend over large regions of intermolecular contacts (Fig. 5b). In species **A**, we observed round, highly localized blue color NCI[72,73] domains in the region where oxygen and hydrogen interact (O1—H1), followed by a vastly scattered region representing weak van der Waals interactions between O1–H2, O1–H3, and O1–H4. In species **A**, the partial charges on the hydrogen atoms involved in H-bonds ranged from +0.25 to +0.29 au, while a large positive

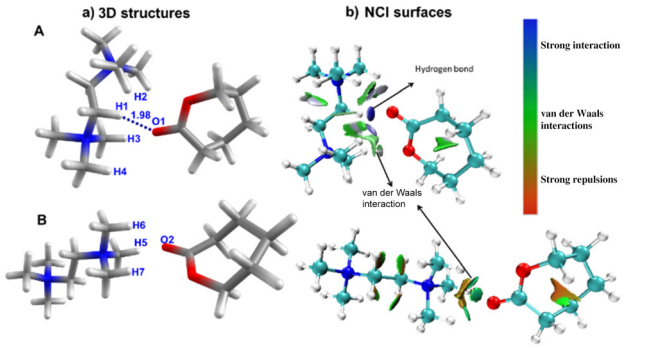

Fig. 5 (a) Molecular modelling of complexes between the cationic catalyst and ε-CL in different orientations of these species (A and B) (b) NCI surfaces (iso value = 0.5). Color code: C (black), O (red), H (grey), and N (blue).

charge of +0.82 au on the C atom of the (C═O) of ε-CL indicates higher electrophilicity.

On the other hand, the NCI plot of species **B** does not reveal any hydrogen bonding interaction, which agrees with the structural topology. In addition, we have performed energy decomposition analysis (EDA)[74] on species **A** and **B** by fragmenting them in quarternary ammonium dicationic salt and ε-CL (see the ESI† for details). The total intermolecular interaction computed total interaction energies (ΔE_{int}) are −38.3 and −31.1 kcal mol^{-1} for species **A** and **B**, respectively, indicating that the former species is stabilized by ∼7 kcal mol^{-1} compared to species **B**. The decomposed energy shows that the significant contribution emerges from electrostatic interactions, followed by Pauli (repulsive in nature) and orbital interactions. Due to hydrogen bonding interactions, we observed relatively higher electrostatic and orbital interaction energies in species **A** than in species **B**. The steric repulsion (Pauli) is relatively large in species **A**, due to the large number of protons close to ε-CL. Moreover, the dispersion interactions are more robust in species **A** than in species **B**.

The recyclability and reusability features of the catalyst were also assessed in terms of its possible application in the industry. It was studied for the ROP of ε-CL (100 equivalent) under the standard reaction conditions (Table 3). After the polymerization (8 h), the entire reaction mixture was added dropwise to water, where PCL was precipitated as a solid, and the catalyst was dissolved in water. The polymer was then isolated from water by a simple filtration technique. The filtrate containing the catalyst was evaporated to recover and reuse the catalyst for

Table 3 Recyclability and reusability of *N,N′*-dibutyl-*N,N,N′*, *N′*-tetramethylethane-1,2-diammonium bromide in the ROP of ε-CL[a]

# of cycles	1	2	3	4	5	6
Conv[b] (%)	98	97.7	97.8	97.0	97.2	97.1
M_{nexp}[c] (kDa)	11.0	11.2	11.2	10.9	11.3	11.1
PDI[c]	1.1	1.3	1.3	1.3	1.3	1.2

[a] Reaction conditions: 60 °C, toluene (solvent), 8 h, $[M]_0/[cat]_0 = 100:1$. [b] Determined by ^{1}H NMR. [c] Determined by GPC.

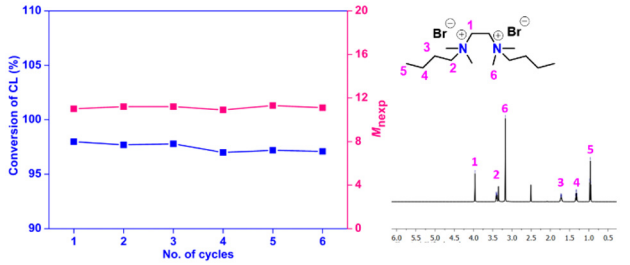

Fig. 6 (a) Recycling studies of *N*,*N*′-dibutyl-*N*,*N*,*N*′,*N*′-tetramethylethane-1,2-diammonium bromide as the catalyst for the ROP of ε-CL and (b) ^{1}H NMR spectra of the catalyst after 6th cycle.

the next cycle. The process was repeated for up to five cycles while keeping the initial catalyst-to-monomer ratio at 1 : 100, and the results are summarized in Table 3 and Fig. 6. Remarkably, about 95% of the used catalyst could be recovered in the first cycle and reused up to six successive cycles of reaction without substantial loss in catalytic efficiency (Table TS3 in the ESI†). The gradual drop in catalyst recovery in the subsequent cycles is considered mainly due to the difficulty associated with handling of smaller mass of the catalyst in the lab setup. The solvent recovery study carried out using a higher-scaled reaction (~10×) indicated about 95% recovery of toluene after the reaction (Table TS2 in the ESI†).

The catalytic performance of the supported organocatalysts generally shows a noticeable drop after a few cycles because of their intrinsic defects, such as the loss of attached organocatalysts from the supports or the mass transfer of the reactants to the supports.[75,76] However, the polymerization was under outstanding control in the present case, affording PCL with the expected molecular weight and narrow dispersity in each cycle (Table 3). To further substantiate the result, the recycled catalyst obtained after the 6th cycle was analyzed by ^{1}H NMR (Fig. 6b) and the spectra revealed no change before and after the recyclability experiment, indicating that the catalyst remains reasonably stable even after six cycles.

Conclusions

In summary, *N*,*N*′-dibutyl-*N*,*N*,*N*′,*N*′-tetramethylethane-1,2-diammonium bromide was investigated to exhibit its catalytic performance in the ROP of ε-CL at 60 °C. Efficient ROP was demonstrated with very good control over the polymerization without an external initiator. To the best of our knowledge, this is the first report on organocatalyzed cyclic ester ROP accomplished without using an external initiator. Various well-defined PCLs with precisely controlled M_n were successfully synthesized and characterized with NMR, GPC, TGA, and DSC. The fact that the catalyst can be easily recovered and reused without the loss of catalytic activity makes this catalyst an attractive recyclable organocatalyst for preparing biodegradable polyesters, avoiding the tedious and uneconomical heterogeneous catalyst fabrication process.

Author contributions

Shweta Sagar: methodology, data curation, formal analysis, software, and writing – original draft. Shiva Lall Sunar: catalyst synthesis and analysis. Priyanku Nath: data curation and formal analysis. Aranya Ray: data curation and formal analysis. Mridula Choudhary: DFT calculation and data analysis. Saurabh K. Singh: DFT calculation and data analysis. Alok Sarkar: supervision and writing – review & editing. Tarun K. Panda: conceptualization, supervision, project administration, resources, and writing – review & editing.

Data availability

All the data used in this work are available in the ESI and the references cited in the manuscript.†

Conflicts of interest

There are no conflicts to declare.

Acknowledgements

The authors appreciate the financial support from SERB, India under project no. CRG/2022/001941. The Department of Chemistry at IIT Hyderabad is acknowledged for its instrumental facilities. S. S. acknowledges the Prime Minister's Research Fellowship (2000829) for financial assistance. P. N. and S. L. S. thank CSIR (09/1001(15565)/2022-EMR-I and 09/1001(0090)/2021-EMR-I) for their PhD fellowships. A. R. and M.C. thank MHRD and UGC for their PhD fellowships. Part of the graphical abstract images is designed by brgfx / Freepik.

References

1 C. Bissantz, B. Kuhn and M. Stahl, *J. Med. Chem.*, 2010, **53**, 5061–5084.
2 H. J. Böhm and G. Schneider, *Protein-ligand interactions from molecular recognition to drug design*, Wiley-VCH, 2003.
3 J. W. Steed, J. L. Atwood and P. A. Gale, in *Supramolecular Chemistry*, Wiley, 2012.
4 H. J. Schneider, *Angew. Chem., Int. Ed.*, 2009, **48**, 3924–3977.
5 M. Shahinpoor, *Polymer Sensors and Actuators*, Springer Berlin Heidelberg, 2000.
6 J. J. Shea, *IEEE Electr. Insul. Mag.*, 2005, **15**, 50–51.
7 S. E. Wheeler, T. J. Seguin, Y. Guan and A. C. Doney, *Acc. Chem. Res.*, 2016, **49**, 1061–1069.
8 G. A. Jeffrey and G. A. Jeffrey, *An introduction to hydrogen bonding*, Oxford University Press, New York, 1997, vol. 12.
9 J. N. Israelachvili, *Intermolecular and Surface Forces*, Elsevier, 2011.

10 E. A. Meyer, R. K. Castellano, F. Diederich, R. K. Castellano, F. Diederich and E. A. Meyer, *Angew. Chem., Int. Ed.*, 2003, **42**, 1210–1250.
11 J. C. Ma, D. A. Dougherty and M. Beckman, *Chem. Rev.*, 1997, **97**(5), 1303–1324.
12 C. Tanford, *Science*, 1978, **200**, 1012–1018.
13 L. Pauling, *Chem. Eng. News*, 1946, **24**(10), 1375–1377.
14 A. Warshel, P. K. Sharma, M. Kato, Y. Xiang, H. Liu and M. H. M. Olsson, *Chem. Rev.*, 2006, **106**, 3210–3235.
15 W. Zhao, Y. Lv, J. Li, Z. Feng, Y. Ni and N. Hadjichristidis, *Nat. Commun.*, 2019, **10**(1), 3590.
16 M. Labet and W. Thielemans, *Chem. Soc. Rev.*, 2009, **38**, 3484–3504.
17 Data Bridge Market Research, **https://markets.businessinsider.com/news/stocks/polycaprolactone-pcl-market-destine-to-reach-usd-909-81-billion-with-an-excellent-cagr-of-10-50-by-2029-1032246582** (accessed on 30th March 2024).
18 C. Jérôme and P. Lecomte, *Adv. Drug Delivery Rev.*, 2008, **60**, 1056–1076.
19 H. Zhang, Y. Dong, K. Huang, J. Liu, B. Dong and F. Wang, *Eur. Polym. J.*, 2019, **118**, 633–641.
20 H. C. Huang, B. Wang, Y. P. Zhang and Y. S. Li, *Polym. Chem.*, 2016, **7**, 5819–5827.
21 R. Olejník, M. Bílek, Z. Růžičková, Z. Hoštálek, J. Merna and A. Růžička, *J. Organomet. Chem.*, 2015, **794**, 237–246.
22 D. J. Darensbourg and O. Karroonnirun, *Macromolecules*, 2010, **43**, 8880–8886.
23 V. Paradiso, V. Capaccio, D. H. Lamparelli and C. Capacchione, *Coord. Chem. Rev.*, 2021, **429**, 213644.
24 J. Chen, X. Wu, L. Zhang, Z. Duan and B. Liu, *Polym. Chem.*, 2022, **13**, 2971–2979.
25 S. Sagar, H. Karmakar, P. Nath, A. Sarkar, V. Chandrasekhar and T. K. Panda, *Chem. Commun.*, 2023, **59**(56), 8727–8730.
26 S. Sagar, K. Bano, A. Sarkar, K. Pal and T. K. Panda, *Eur. J. Inorg. Chem.*, 2022, **34**, e202200494.
27 A. C. Albertsson and I. K. Varma, *Biomacromolecules*, 2003, **4**, 1466–1486.
28 S. Binauld and M. H. Stenzel, *Chem. Commun.*, 2013, **49**, 2082–2102.
29 R. A. Qazi, M. S. Khan, L. A. Shah, R. Ullah, A. Kausar and R. Khattak, *Polym.-Plast. Technol. Mater.*, 2020, **59**, 928–951.
30 B. Guo and P. X. Ma, *Sci. China: Chem.*, 2014, **57**, 490–500.
31 K. Fukushima and K. Nozaki, *Macromolecules*, 2020, **53**, 5018–5022.
32 C. J. Zhang and X. H. Zhang, *Sci. China: Chem.*, 2019, **62**, 1087–1089.
33 M. Nikulin and V. Švedas, *Molecules*, 2021, **26**(09), 2750.
34 V. Blanco, D. A. Leigh and V. Marcos, *Chem. Soc. Rev.*, 2015, **44**, 5341–5370.
35 S. I. Shoda, H. Uyama, J. I. Kadokawa, S. Kimura and S. Kobayashi, *Chem. Rev.*, 2016, **116**, 2307–2413.
36 R. A. Gross, A. Kumar and B. Kalra, *Chem. Rev.*, 2001, **101**, 2097–2124.
37 C. Thomas, F. Peruch, A. Deffieux, A. Milet, J. P. Desvergne and B. Bibal, *Adv. Synth. Catal.*, 2011, **353**, 1049–1054.
38 J. Liu, C. Chen, Z. Li, W. Wu, X. Zhi, Q. Zhang, H. Wu, X. Wang, S. Cui and K. Guo, *Polym. Chem.*, 2015, **6**, 3754–3757.
39 A. Alba, A. Schopp, A. P. De Sousa Delgado, R. Cherif-Cheikh, B. Martín-Vaca and D. Bourissou, *J. Polym. Sci., Part A: Polym. Chem.*, 2010, **48**, 959–965.
40 S. Koeller, J. Kadota, A. Deffieux, F. Peruch, S. Massip, J. M. Léger, J. P. Desvergne and B. Bibal, *J. Am. Chem. Soc.*, 2009, **131**, 15088–15089.
41 G. Gontard, A. Amgoune and D. Bourissou, *J. Polym. Sci., Part A: Polym. Chem.*, 2016, **54**, 3253–3256.
42 O. I. Kazakov and M. K. Kiesewetter, *Macromolecules*, 2015, **48**, 6121–6126.
43 O. I. Kazakov, P. P. Datta, M. Isajani, E. T. Kiesewetter and M. K. Kiesewetter, *Macromolecules*, 2014, **47**, 7463–7468.
44 F. Shi, Y. Gu, Q. Zhang and Y. Deng, *Catal. Surv. Asia*, 2004, **8**(3), 179–186.
45 Y. Li, S. Hu, J. Cheng and W. Lou, *Chin. J. Catal.*, 2014, **35**, 396–406.
46 L. Zhang, M. Xian, Y. He, L. Li, J. Yang, S. Yu and X. Xu, *Bioresour. Technol.*, 2009, **100**, 4368–4373.
47 P. Naert, K. Rabaey and C. V. Stevens, *Green Chem.*, 2018, **20**, 4277–4286.
48 M. Vafaeezadeh and M. M. Hashemi, *J. Chem. Eng.*, 2014, **250**, 35–41.
49 R. Kore and R. Srivastava, *J. Mol. Catal. A: Chem.*, 2013, **376**, 90–97.
50 A. Kaoukabi, F. Guillen, H. Qayouh, A. Bouyahya, S. Balieu, L. Belachemi, G. Gouhier and M. Lahcini, *Ind. Crops Prod.*, 2015, **72**, 16–23.
51 N. Cheechana, W. Benchaphanthawee, N. Akkravijitkul, P. Rithchumpon, T. Junpirom, W. Limwanich, W. Punyodom, N. Kungwan, C. Ngaojampa, P. Thavornyutikarn and P. Meepowpan, *Polymers*, 2021, **13**, 4290.
52 M. C. Bubalo, K. Radošević, I. R. Redovniković, I. Slivac and V. G. Srček, *Arh. Hig. Rada Toksikol.*, 2017, **68**, 171–179.
53 S. K. Singh and A. W. Savoy, *J. Mol. Liq.*, 2020, **297**, 112038.
54 B. Jastorff, R. Störmann, J. Ranke, K. Mölter, F. Stock, B. Oberheitmann, W. Hoffmann, J. Hoffmann, M. Nüchter and B. Ondruschka, *Green Chem.*, 2003, **5**, 136–142.
55 R. Kawai, S. Yada and T. Yoshimura, *ACS Omega*, 2019, **4**, 14242–14250.
56 R. Zana, *J. Colloid Interface Sci.*, 2002, **248**, 203–220.
57 R. Zana, *Curr. Opin. Colloid Interface Sci.*, 1996, **1**, 566–571.
58 K. Fukushima, D. Tabuani, C. Abbate, M. Arena and P. Rizzarelli, *Eur. Polym. J.*, 2011, **47**, 139–152.
59 K. Makiguchi, Y. Ogasawara, S. Kikuchi, T. Satoh and T. Kakuchi, *Macromolecules*, 2013, **46**, 1772–1782.
60 N. Zhu, Y. Liu, J. Liu, J. Ling, X. Hu, W. Huang, W. Feng and K. Guo, *Sci. Rep.*, 2018, **8**, 3734.
61 Y. Zhao, X. Lim, Y. Pan, L. Zong, W. Feng, C. H. Tan and K. W. Huang, *Chem. Commun.*, 2012, **48**, 5479–5481.
62 D. Delcroix, A. Couffin, N. Susperregui, C. Navarro, L. Maron, B. Martin-Vaca and D. Bourissou, *Polym. Chem.*, 2011, **2**, 2249–2256.

63 X. Zhi, J. Liu, Z. Li, H. Wang, X. Wang, S. Cui, C. Chen, C. Zhao, X. Li and K. Guo, *Polym. Chem.*, 2016, **7**, 339–349.
64 A. Buchard, D. R. Carbery, M. G. Davidson, P. K. Ivanova, B. J. Jeffery, G. I. Kociok-Köhn and J. P. Lowe, *Angew. Chem., Int. Ed.*, 2014, **53**, 13858–13861.
65 M. K. Kiesewetter, E. J. Shin, J. L. Hedrick and R. M. Waymouth, *Macromolecules*, 2010, **43**, 2093–2107.
66 P. Li, Y. Xi, L. Li, H. Li, W. H. Sun and M. Lei, *Inorg. Chim. Acta*, 2018, **477**, 34–39.
67 J. Martínez, J. F. Cortés and R. Miranda, *Processes*, 2022, **10**, 1274.
68 S. Mandal, R. Narvariya, S. L. Sunar, I. Paul, A. Jain and T. K. Panda, *Green Chem.*, 2023, **25**, 8266–8272.
69 C. Lee, E. Yang and R. G. Parr, *Phys. Rev. B: Condens. Matter Mater. Phys.*, 1988, **37**, 785.
70 A. D. Becke, *J. Chem. Phys.*, 1993, **98**, 5648–5652.
71 W. J. Hehre, K. Ditchfield and J. A. Pople, *J. Chem. Phys.*, 1972, **56**, 2257–2261.
72 E. R. Johnson, S. Keinan, P. Mori-Sánchez, J. Contreras-García, A. J. Cohen and W. Yang, *J. Am. Chem. Soc.*, 2010, **132**, 6498–6506.
73 J. Contreras-García, E. R. Johnson, S. Keinan, R. Chaudret, J. P. Piquemal, D. N. Beratan and W. Yang, *J. Chem. Theory Comput.*, 2011, **7**, 625–632.
74 L. Zhao, M. von Hopffgarten, D. M. Andrada and G. Frenking, *Wiley Interdiscip. Rev.: Comput. Mol. Sci.*, 2018, **8**, e1345.
75 O. Gleeson, G. L. Davies, A. Peschiulli, R. Tekoriute, Y. K. Gun'Ko and S. J. Connon, *Org. Biomol. Chem.*, 2011, **9**, 7929–7940.
76 U. Yolsal, T. A. R. Horton, M. Wang and M. P. Shaver, *Prog. Polym. Sci.*, 2020, **111**, 101313.

